

Time-resolved spectroscopy of 3-amino-tetrazine and 3-amino-6-methyl-tetrazine in a supersonic jet

Joseph C. Alfano, Selso J. Martinez III, and Donald H. Levy

Citation: *The Journal of Chemical Physics* **94**, 2475 (1991); doi: 10.1063/1.459871

View online: <http://dx.doi.org/10.1063/1.459871>

View Table of Contents: <http://scitation.aip.org/content/aip/journal/jcp/94/4?ver=pdfcov>

Published by the AIP Publishing

Articles you may be interested in

[Electronic Spectroscopy of Biological Molecules in Supersonic Jets: The Amino Acid Tryptophane](#)
AIP Conf. Proc. **1084**, 539 (2008); 10.1063/1.3076535

[Vibrational predissociation in argon complexes of 3-aminotetrazine and 3-amino-6-methyltetrazine: Evidence for extreme mode selectivity](#)
J. Chem. Phys. **96**, 2522 (1992); 10.1063/1.462004

[The electronic spectroscopy and structure of complexes of argon with 3-aminotetrazine in a supersonic jet](#)
J. Chem. Phys. **94**, 1673 (1991); 10.1063/1.459939

[The spectroscopy of dimethyltetrazine cooled in a supersonic free jet](#)
J. Chem. Phys. **81**, 2270 (1984); 10.1063/1.447927

[Stroboscopic Time-Resolved Spectroscopy](#)
Rev. Sci. Instrum. **36**, 37 (1965); 10.1063/1.1719320



Time-resolved spectroscopy of 3-amino-*s*-tetrazine and 3-amino-6-methyl-*s*-tetrazine in a supersonic jet

Joseph C. Alfano, Selso J. Martinez III, and Donald H. Levy

The James Franck Institute and the Department of Chemistry, The University of Chicago, Chicago, Illinois 60637

(Received 30 October 1990; accepted 15 November 1990)

Time-resolved measurements have been performed on seven vibronic levels of the S_1 states of 3-amino-*s*-tetrazine (AT) and nine vibronic levels of 3-amino-6-methyl-*s*-tetrazine (AMT) ranging from 0 to 1907 cm^{-1} of excess vibrational energy. The resulting fluorescence lifetimes were found to range from 219 to 59 ns, and monotonically decreased with increasing excess energy. We have estimated the nonradiative rates and fluorescence quantum yields for these 16 levels by two different methods, which give reasonable agreement. These show that AT and AMT have nonradiative rates around $10^6\text{--}10^7\text{ s}^{-1}$, and very high fluorescence quantum yields, ranging from 0.07 to 0.29. This stands in contrast to *s*-tetrazine, which has a fluorescence lifetime of 800 ps, a nonradiative rate of $1.25 \times 10^9\text{ s}^{-1}$, and a fluorescence quantum yield of 0.000 94. This difference in the photophysical properties of AT and AMT relative to tetrazine is discussed in terms of the extensive work done on the photophysics and substituent effects of other azabenzenes, particularly pyridine.

I. INTRODUCTION

The photophysics and photochemistry of *s*-tetrazine in its \tilde{A}^1B_3 state has been an active area of research in recent years.¹⁻¹⁶ Since the earliest work by Chowdhury *et al.*¹⁷ and Vemulapalli *et al.*,¹⁸ it has been realized that \tilde{A}^1B_{3u} tetrazine has an efficient nonradiative decay pathway, resulting in a very short lifetime and an exceedingly small fluorescence quantum yield. Hochstrasser *et al.*^{8,9} deduced that tetrazine undergoes efficient photodissociation to form two HCN molecules and N_2 , and that the rate limiting step for the photodissociation was internal conversion of the optically prepared \tilde{A}^1B_{3u} state to the \tilde{X}^1A_g state. The dissociation then proceeds along the \tilde{X}^1A_g ground state surface. Other groups in recent years have undertaken additional studies of the details of the photodissociation process.^{3,15} The fluorescence lifetime of vibrationless \tilde{A}^1B_{3u} *s*-tetrazine in a supersonic jet is 800 ps,^{16,19,20} and the fluorescence quantum yield is 0.000 94.¹⁶ Time-resolved measurements have also been performed on methyltetrazine (MT) and dimethyltetrazine (DMT).²¹

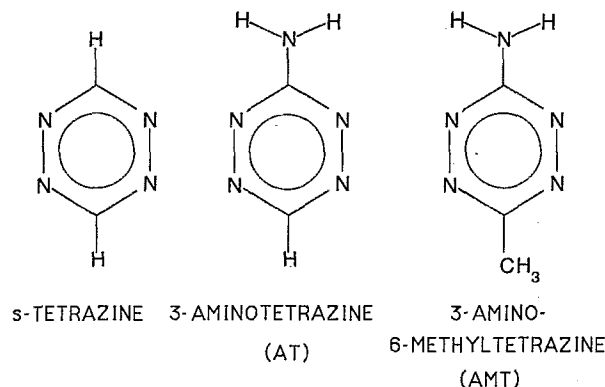
Recently, we have become interested in the molecules 3-amino-*s*-tetrazine (AT) and 3-amino-6-methyl-*s*-tetrazine (AMT), shown in Fig. 1. We investigated²² the photodissociation dynamics of van der Waals complexes of AT and AMT with argon atoms. We found evidence of striking mode selectivity, where the photodissociation rate varied by a factor of 200 among various initially excited vibrational modes. Additionally, the branching ratio between the two possible photoproducts of the di-argon complex showed large mode selectivity.

In an effort to understand this puzzling behavior, we performed a detailed study of the structure and spectroscopy of AT, AMT, and their argon clusters.^{23,24} During the course of these experiments, we noticed that at vapor pressures sufficient to produce strong fluorescence signals, our limited samples of AT and AMT lasted for a very long time. This suggested that the concentrations of AT and

AMT in the jet were very much less than concentrations used in previous tetrazine experiments, and this in turn suggested that the fluorescence quantum yields of AT and AMT were much higher than the 0.000 94 quantum yield of tetrazine. Hence, we attempted to measure the fluorescence lifetimes of various vibrational levels of these molecules using nanosecond lasers. To our surprise, we found that the vibrational levels of AT and AMT have extremely long fluorescence lifetimes, ranging up to a factor of 300 longer than corresponding levels in tetrazine. In this paper we describe these measurements and report the lifetimes of 16 vibrational levels of AT and AMT. We also obtain estimates from two independent methods of the radiative rate, nonradiative rate, and fluorescence quantum yield of these levels. Finally, we discuss the reason for the large differences in nonradiative rates and quantum yields between AT, AMT, and tetrazine in terms of previous work on the excited state photophysics of other azabenzenes.

II. EXPERIMENT

The basic experimental apparatus has been described elsewhere,^{25,26} and only a brief description will be given here. An AT or AMT seeded supersonic jet was generated by passing helium through a reservoir containing the respective molecule heated to 85°C , and then expanding the mixture through a $100\text{ }\mu\text{m}$ pinhole. The supersonic jet was crossed by the output of a Nd:Yag pumped dye laser, operating with either Fluorescein 548 or Coumarin 500. The resulting fluorescence was imaged onto a slit by a quartz lens, which served to limit scattered laser light, and was detected by an RCA 8575 photomultiplier tube. The output of the photomultiplier tube was sent to a transient digitizer with a 10 ns/bin digitization rate. The digitizer was interfaced to a Dell 310 computer via a CAMAC dataway. The laser pulse width was about 7 ns FWHM,

FIG. 1. The *s*-tetrazine, AT, and AMT molecules.

and our instrument response function, measured by scattering laser light off the jet nozzle, was found to be approximately 20 ns FWHM.

The fluorescence decays were fit using the method of iterative convolutions.²⁷ All decays were well fit by single exponential functions. The quality of the fit was judged by the χ^2 criterion, and by visual inspection for systematic deviations of the residuals. For weak transitions, the first 30 ns of the decay were not fit, to eliminate contributions from scattered laser light. The solution absorption experiments were done using a Perkin-Elmer Model 330 UV-VIS spectrophotometer.

III. RESULTS

A. AT fluorescence lifetimes

Using our nanosecond time-resolved setup described in the previous section, we have measured the fluorescence lifetimes of seven vibronic levels of AT, and Fig. 2 shows a typical decay along with the instrument response function and our best convoluted fit, in this case for the AT zero-

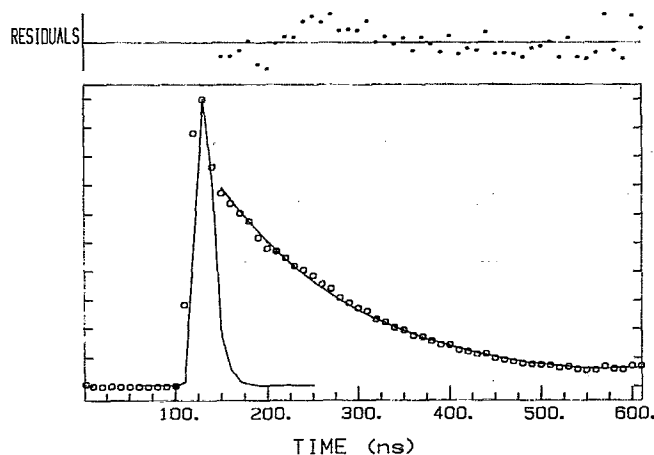


FIG. 2. The fluorescence decay (circles) and the best least-squares convoluted fit (solid line through circles) of the origin level of AT, which has a lifetime of 154 ± 5 ns. The instrument response function is also shown, as are the residuals.

TABLE I. Fluorescence lifetimes, nonradiative rates, and fluorescence quantum yields of various AT vibronic levels.

Level	$\Delta\nu(\text{cm}^{-1})^a$	$\tau(\text{ns})^b$	Method 1 ^c		Method 2 ^d	
			$k_{\text{nr}}(\times 10^{-6})$	ϕ_{fl}	$k_{\text{nr}}(\times 10^{-6})$	ϕ_{fl}
0 ⁰	0	154	2.7	0.59	5.4	0.18
16b ²	429	143	3.2	0.54	5.9	0.16
16a ²	505	103	5.9	0.39	8.6	0.12
6a ¹	606	90	7.3	0.34	10.0	0.10
1 ¹	798	85	8.0	0.32	10.6	0.10
6a ²	1212	62	12.3	0.24	13.8	0.07
6a ¹ 1 ¹	1404	59	13.1	0.22	15.8	0.07

^a $\Delta\nu$ is a given relative to the AT origin transition at $18\,410\text{ cm}^{-1}$.

^bUncertainty is estimated to be ± 5 ns, except for the 16b² level which is estimated to be ± 10 ns.

^cMethod 1, as described in the text, makes use of a radiative lifetime of 263 ± 20 ns. The uncertainties in k_{nr} and ϕ_{fl} are estimated at $\pm 10\%$.

^dMethod 2 used a value of 880 ± 80 ns for τ_{rad} , as determined from solution absorption measurements. Uncertainties in k_{nr} and ϕ_{fl} are estimated to be $\pm 10\%$.

point level. The 154 ns lifetime of this decay is much longer than our instrument response function (20 ns FWHM) and hence the lifetimes can easily be measured with nanosecond lasers.

The fluorescence lifetimes of seven vibronic features of AT are listed in Table I. All decays were fit well by single exponential functions. The lifetime of the zero-point level of AT is 154 ± 5 ns, and the fluorescence lifetimes of the excited vibrational levels decrease smoothly and monotonically with increasing energy to 59 ± 5 ns for the 6a¹1¹ level at $+1406\text{ cm}^{-1}$. Thus the fluorescence lifetimes of the vibronic levels of AT are more than two orders of magnitude larger than the corresponding levels of tetrazine.^{16,19,20} The fluorescence lifetimes and, by implication, the rate of any nonradiative process appear to depend only on the amount of excess vibrational energy, and not on the nature of the initially excited vibrational mode of AT. This is different from tetrazine, where significant mode selectivity was observed.³¹

B. AMT fluorescence lifetimes

We have obtained the fluorescence lifetimes of nine vibronic levels of AMT, and these are shown in the third column of Table II. All decays were fit well by single exponentials. In Fig. 3, we show a typical decay, and the best least-squares convolution fit, in this case for the 16b² level of AMT. For the weaker transitions, like 16b², there is a significant amount of scattered laser light at early times in the decay, and therefore in our fit we truncate the early channels and only use data points occurring 30 ns or more after the laser pulse. As all decays are longer than about 60 ns, we are able to do this without losing much of the decay profile.

The lifetime of the zero-point level of AMT is 219 ± 5 ns, and the lifetimes decrease smoothly and monotonically with excess energy to 63 ± 5 ns for the 6a²1¹ level at $+1907\text{ cm}^{-1}$ excess vibrational energy. The lifetimes of these levels are about 40% larger than the corresponding levels in AT, and over a factor of 250 larger than the

TABLE II. Fluorescence lifetimes, nonradiative rates, and fluorescence quantum yields of various AMT vibronic levels.

Level	$\Delta\nu(\text{cm}^{-1})^a$	$\tau(\text{ns})^b$	Method 1 ^c		Method 2 ^d	
			$k_{\text{nr}}(\times 10^{-6})$	ϕ_{fl}	$k_{\text{nr}}(\times 10^{-6})$	ϕ_{fl}
0^0	0	219	0.8	0.83	3.3	0.29
$16b^2$	266	184	1.6	0.70	4.1	0.24
$16a^2$	478	155	2.7	0.59	5.1	0.20
$6a^1$	530	117	4.7	0.44	7.2	0.15
1^1	849	120	4.5	0.46	7.0	0.16
$6a^2$	1059	93	7.0	0.35	9.4	0.12
$6a^11^1$	1378	80	8.7	0.30	11.2	0.11
$6a^3$	1587	69	10.7	0.26	13.2	0.09
$6a^21^1$	1907	63	12.1	0.24	14.6	0.07

^a $\Delta\nu$ is given relative to the AMT origin transition at $18\,024\text{ cm}^{-1}$.

^bUncertainty is estimated to be $\pm 5\text{ ns}$.

^cMethod 1, as described in the text, makes use of a radiative lifetime of $263 \pm 20\text{ ns}$. The uncertainties in k_{nr} and ϕ_{fl} are estimated at $\pm 10\%$.

^dMethod 2 used a value of $760 \pm 80\text{ ns}$ for τ_{rad} , as determined from solution absorption measurements. Uncertainties in k_{nr} and ϕ_{fl} are estimated to be $\pm 10\%$.

lifetimes of the corresponding tetrazine levels. Once again the sensitivity of the fluorescence lifetimes to the initially excited vibrational mode seen in tetrazine is not observed here. Instead, the fluorescence lifetime appears to be a function only of the excess vibrational energy.

C. Solution absorption spectra

The lifetimes of AT and AMT relative to tetrazine are exceptionally long, and extracting the fluorescence quantum yields and radiative rates is a problem of considerable interest. In Sec. IV, we describe two ways of obtaining this information. One method depends on determining the radiative rate from integration of the solution absorption spectrum, and the solution phase absorption spectra of AT and AMT in benzene are shown in Figs. 4 and 5. Both molecules show a transition to a lower electronic state centered at about 535 nm, with $\epsilon_{\text{max}} = 700$ at 534 nm for AT,

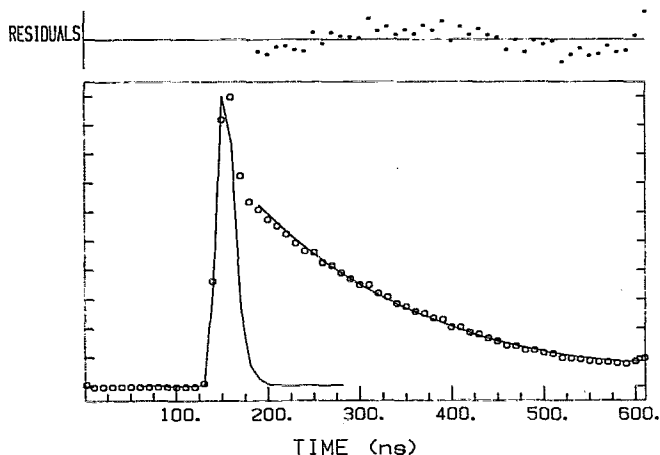


FIG. 3. The fluorescence decay (circles) and the best least-squares convoluted fit (solid line through circles) of the $16b^2$ level of AMT, which has a lifetime of $184 \pm 5\text{ ns}$. The instrument response function is also shown, as are the residuals.

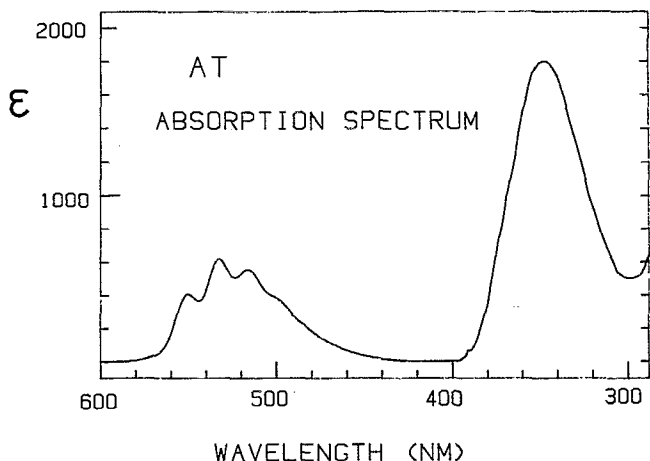


FIG. 4. The solution absorption spectrum of AT in benzene, taken at a resolution of 1 nm, and a concentration of $4.5 \times 10^{-4}\text{ M}$. The S_1 transition is centered at about 535 nm, while the feature at about 350 nm is the S_2 state.

and $\epsilon_{\text{max}} = 640$ at 526 nm for AMT. This transition is the $\pi^* \leftarrow n$ to the lowest excited singlet state, the transition studied in our previous work. Some vibrational structure corresponding to the $6a$ vibrational mode can be seen, and this structure becomes better resolved when the spectra are taken in hexane. Unfortunately AT and AMT are not sufficiently soluble in hexane, and we were unable to do quantitative work in this solvent. At high energies, one sees a second transition centered at about 350 nm, with $\epsilon_{\text{max}} = 1830$ at 346 nm for AT, and $\epsilon_{\text{max}} = 2310$ at 352 nm for AMT. This transition is structureless in benzene, but in hexane we see some structure, apparently caused by a vibration of about 1100 cm^{-1} . This higher energy electronic state is evidently a second $\pi^* \leftarrow n$ state, corresponding to what Schaefer has identified⁶ as the $\tilde{A}^1B_{3u}(\pi^* \leftarrow n)$ transition in tetrazine, which was observed by Mason³⁰ at 320 nm in cyclohexane.

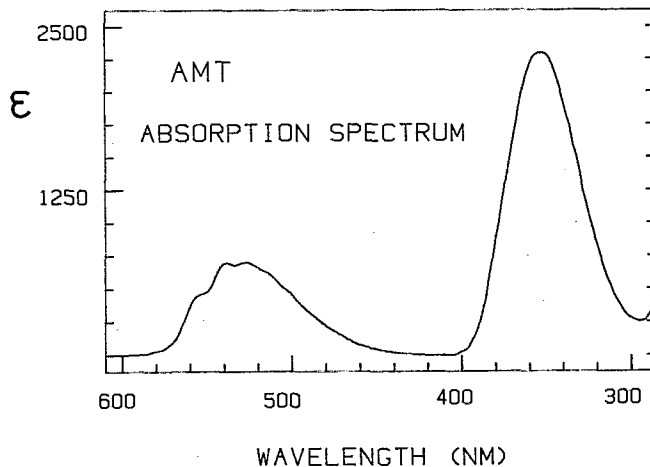


FIG. 5. The solution absorption spectrum of AMT in benzene, taken at a resolution of 1 nm, and a concentration of $3.5 \times 10^{-4}\text{ M}$. The S_1 transition is centered at about 540 nm, while the feature at about 350 nm is the S_2 state.

TABLE III. Fluorescence lifetimes, nonradiative lifetimes, and fluorescence quantum yields for tetrazine and its various derivatives in their zero-point levels.

Molecule	$\tau_{\text{fl}}(\text{ns})$	$\tau_{\text{rad}}(\text{ns})$	k_{nr}	ϕ_{fl}
Tetrazine	0.8 ^a	850 ^b	1.2×10^9	0.000 94
MT	3.1 ^c	850 ^d	3.2×10^8	0.003 7
DMT	9.5 ^c	850 ^d	1.0×10^8	0.011
AT ^e	154	890	5.4×10^6	0.18
AMT ^e	219	760	3.3×10^6	0.29

^aReferences 16, 19, and 20.

^bReferences 31 and 32.

^cReference 21.

^dThe radiative lifetimes for MT and DMT are set equal to that of tetrazine, as described in the text.

^e τ_{rad} , k_{nr} , and ϕ_{fl} for AT and AMT are calculated using method 2, as described in the text.

IV. DISCUSSION

A. Calculation of radiative lifetimes

As can be seen in Table III, the fluorescence lifetimes of AT and AMT are much larger than those of tetrazine and its methyl derivatives. The radiative lifetime of tetrazine is known to be 850 ns,^{31,32} and therefore the 800 ps fluorescence lifetime of the tetrazine origin level corresponds to a fluorescence quantum yield of 0.000 94. The long fluorescence lifetimes of AT and AMT indicate that in these molecules nonradiative processes are much less efficient than in tetrazine, and the fluorescence quantum yields must be correspondingly large. We would like to quantify this argument and extract the radiative rates and quantum yields of the various vibronic levels of jet-cooled AT and AMT. The most definitive method of doing so is to perform an absorption experiment in a jet. However, a jet absorption experiment requires a much higher concentration of AT and AMT in the beam than a fluorescence experiment, and our very limited supply of sample did not enable us to run at temperatures necessary to generate such a high vapor pressure. Hence, we have made use of two independent methods to obtain estimates of the quantum yields and nonradiative rates of the AT and AMT vibronic levels. There is reasonable agreement between the two methods.

1. Method 1

We initially attempted to estimate the AT and AMT quantum yields and nonradiative rates by making use of the data available from tetrazine and its methyl derivatives. The radiative lifetime of tetrazine is known to be 850 ns. If we make the assumption that placing a methyl group onto the tetrazine ring does not change the radiative lifetime, we can obtain the quantum yields and nonradiative rates for the origin levels of methyltetrazine (MT) and dimethyltetrazine (DMT), which are shown in Table III. The nonradiative rates decrease with increasing methyl substitution. The first methyl group reduces the nonradiative rate by a factor of 3.9, while adding a second methyl substituent further reduces the rate by a factor of 3.1. Thus, the effects of the methyl groups appear to be additive and independent. We make the assumption, which is the core of this

method of analysis, that a methyl substituent reduces the nonradiative rate by a factor of 3.5 ± 0.5 , and hence the nonradiative rate (k_{nr}) of AMT is a factor of 3.5 ± 0.5 less than that of AT. If we further assume that the radiative rates of AT and AMT are equal, then we can set up the following set of simultaneous equations for the origin levels of AT and AMT:

$$k_{\text{fl}}(\text{AT}) = k_{\text{rad}} + k_{\text{nr}} = 6.49 \times 10^6 \text{ s}^{-1}, \quad (1)$$

$$k_{\text{fl}}(\text{AMT}) = k_{\text{rad}} + k_{\text{nr}}/3.5 = 4.57 \times 10^6 \text{ s}^{-1}. \quad (2)$$

These equations can be solved to yield $k_{\text{rad}} = (3.8 \pm 0.3) \times 10^6 \text{ s}^{-1}$ and $k_{\text{nr}} = (2.2 \pm 0.6) \times 10^5 \text{ s}^{-1}$ for AT. In the Condon approximation, the radiative rate is dependent only on the electronic states involved, and is the same for all vibrational levels. Thus, the radiative lifetimes of all the vibronic levels of AT and AMT 263 ± 20 ns. This value of the radiative lifetime is used to obtain the nonradiative rates and fluorescence quantum yields shown under method 1 in Table I for AT and Table II for AMT.

2. Method 2

To justify the assumptions used to obtain the fluorescence quantum yields and nonradiative rates obtained using method 1, we determined these quantities by a second independent method. We measured the radiative rate of AT and AMT via their solution absorption spectra, and corrected for the index of refraction of the solvent.³⁴ As this can be done independently for AT and AMT, we can test the validity of our previous assumption that AT and AMT have the same radiative rate.

Birks³³ has shown that if there is mirror symmetry between the absorption and emission of a molecule, then the radiative rate is given by

$$k_{\text{rad}} = 1/\tau_{\text{rad}} = 2.88 \times 10^{-9} n^2 \times \int [(2\bar{\nu}_0 - \bar{\nu})^3/\bar{\nu}] \epsilon(\bar{\nu}) d\bar{\nu}, \quad (3)$$

where n is the index of refraction, $\bar{\nu}_0$ is the mirror symmetry point in cm^{-1} , and $\epsilon(\bar{\nu})$ is the extinction coefficient at the wavenumber $\bar{\nu}$. The integral runs over the electronic absorption band. As the electronic transition of interest is well separated from all higher electronic states, we are able to perform this analysis. Evaluating the above expression for the solution absorption spectra of AT and AMT in benzene yields, after correction for the solvent index of refraction,³⁴ a gas phase radiative lifetime of 890 ± 80 and 760 ± 80 ns for AT and AMT, respectively, the primary source of uncertainty being the choice of $\bar{\nu}_0$. The nature of the solvent index of refraction correction is currently a subject of some controversy.³⁵⁻³⁷ We merely note that changing the choice of the correction used in our data analysis does not affect any of the qualitative conclusions of this paper. The lifetimes of AT and AMT differ by only about 15%, which helps support the validity of the assumption we made in the previous section that substituting

a methyl group on a tetrazine ring does not affect the radiative lifetime. The nonradiative rates and fluorescence quantum yields calculated using these values for the radiative rate are shown in Tables I and II, under the heading of method 2.

In comparing the radiative lifetimes obtained via method 1 and method 2, we see that they differ by about a factor of 3, which is reasonable in light of the approximations which went in to each of the analyses. The differences in the radiative lifetimes obtained from the two different methods do not affect in any way the qualitative conclusions that the nonradiative rates of AT and AMT are several orders of magnitude less than those of tetrazine, resulting in extremely large fluorescence quantum yields for AT and AMT. The differences in the radiative lifetimes serve to give an idea of the uncertainties of the analysis caused by the approximations which went into them.

The nonradiative rates increase essentially linearly with excess vibrational energy, with the exception of $16b^2$ in AT, whose value of k_{nr} is about a factor of 1.5 too small. Thus, the nonradiative rate appears to depend only on excess vibrational energy, and does not appear to be sensitive to the nature of the initially excited mode. This is in contrast to the mode specificity of the radiationless transition rate in the low vibrational energy regime ($E_{vib} < 1000 \text{ cm}^{-1}$) seen in other molecules.^{31,38,39}

B. Comparison of AT and AMT to tetrazine and its methyl derivative

As shown in Table III, the quantum yield of the zero-point levels of AT and AMT are 0.18 and 0.29, respectively, much larger than the quantum yields of tetrazine and its methyl derivatives. (We will use the quantum yields and nonradiative rates from method 2 for purpose of this discussion.) Table I shows that the fluorescence quantum yields for AT monotonically decrease from 0.18 for the origin to 0.07 for the $6a^11^1$ level at 1404 cm^{-1} of excess energy. Likewise, for AMT the quantum yields smoothly decrease from 0.29 for the origin to 0.08 for the $6a^21^1$ level at 1907 cm^{-1} . In AT k_{nr} ranges from $5.4 \times 10^6 \text{ s}^{-1}$ for the origin to $1.6 \times 10^7 \text{ s}^{-1}$ for $6a^11^1$, while in AMT it varies from $3.3 \times 10^6 \text{ s}^{-1}$ for the origin to $1.5 \times 10^7 \text{ s}^{-1}$ for $6a^21^1$. By comparison, k_{nr} for the tetrazine zero-point level is $1.25 \times 10^9 \text{ s}^{-1}$, almost three orders of magnitude larger than k_{nr} in the zero-point level of AT or AMT. The radiative lifetimes of AT and AMT are about the same as that of tetrazine, within the accuracy of the two methods used to analyze our data. Thus, AT and AMT display behavior which is qualitatively different from that of tetrazine, MT, and DMT.

The primary nonradiative process in tetrazine is internal conversion. Somehow an amino substituent on a tetrazine ring effects a slowdown in the internal conversion rate, and a consequent increase in the fluorescence quantum yield. It is interesting to compare the nonradiative rate of tetrazine with those of other azabenzenes and to examine the effect of amino substitution on these other azabenzenes. Most azabenzenes have relatively small nonradiative rates

compared to tetrazine, and the dominant nonradiative pathway is intersystem crossing rather than internal conversion. For example, the three dinitroazabenzenes, pyrazine, pyrimidine, and pyridazine, have nonradiative rates that are two orders of magnitude smaller than that of tetrazine.⁴⁰⁻⁴²

The nearest analogue to tetrazine is pyridine, which has a fluorescence quantum yield of 6×10^{-5} and an internal conversion rate of $1.7 \times 10^{10} \text{ s}^{-1}$, about an order of magnitude larger than that of tetrazine.⁴¹⁻⁴⁴ Moreover, as in the case of tetrazine, substitution of an amino group to produce 2-aminopyridine decreases the internal conversion rate^{45,46} by about a factor of 40. Since the photophysics of pyridine has been widely studied, comparisons with pyridine might provide insight into the photophysics of tetrazine and AT.

For many years, the nature of the ultrafast internal conversion in pyridine relative to those of other azabenzenes had been thought to be a solved problem. Pyridine photophysics had been interpreted in terms of the proximity effect,⁴⁷⁻⁵⁰ which states that rapid internal conversion results from having a low-lying $\pi^* \leftarrow \pi$ electronic state very near the $\pi^* \leftarrow n$ state. Vibronic mixing between these two states leads to a large frequency change in the vibronically active out-of-plane modes in the $\pi^* \leftarrow n$ state, which increases the Franck-Condon factors and enables these modes to serve as accepting modes in the internal conversion process. The pyridine $\tilde{B}^1B_2(\pi^* \leftarrow \pi)$ state lies only 3500 cm^{-1} above the $\tilde{A}^1B_1(\pi^* \leftarrow n)$ state, compared to a $S_1 - S_2$ gap ranging from 7000 to 9250 cm^{-1} in the diazo molecules pyrazine, pyrimidine, and pyridazine.⁴² This small energy gap was postulated to result in extensive vibronic mixing between the $S_2^1B_2(\pi^* \leftarrow \pi)$ and $S_1^1B_1(\pi^* \leftarrow n)$ states, as mediated by vibrations of A_2 symmetry. The resulting shift in the potential surface causes a large frequency change in the A_2 vibrations between the ground and electronic states, providing good Franck-Condon factors for internal conversion.

The proximity effect also enabled predictions to be made concerning the effect of substituents on the internal conversion rate.⁵⁰ Electron donating moieties are known to lower the energy of $\pi^* \leftarrow \pi$ states and raise the energy of $\pi^* \leftarrow n$ states. Thus, for chromophores whose lowest electronic transition is $\pi^* \leftarrow n$, adding an electron donating substituent will tend to shrink the gap between the $\pi^* \leftarrow n$ and $\pi^* \leftarrow \pi$ states. This increases the magnitude of the vibronic coupling, which in turn causes a larger change in the vibrational frequency of the vibronically active mode. The net result is an enhancement of the internal conversion rate upon substitution of an electron donating moiety.

Recent experiments,⁵¹ however, have cast serious doubt upon the assertion that efficient internal conversion in pyridine results from the proximity effect. Model calculations predict that if the proximity effect is responsible for the rapid internal conversion in pyridine, then optical excitation of out-of-plane bending modes of A_2 symmetry should effect a dramatic increase in the internal conversion rate, relative to other vibrational modes, since modes of A_2 symmetry are most efficient in vibronically coupling the S_1

and S_2 states. Recently, Villa *et al.*⁵¹ studied the photophysics of a variety of pyridine vibronic levels in a supersonic jet. They observed that vibrational modes of A_2 symmetry are not particularly effective in promoting internal conversion, as would be expected if the proximity effect played an important role in the internal conversion process. They therefore cast doubt upon the previously generally accepted belief that efficient internal conversion in pyridine results from the proximity effect. Villa *et al.* proposed that instead rapid internal conversion may be caused by valence distortion, in which a change in the equilibrium position of the molecule upon electronic excitation results in favorable Franck-Condon factors for transitions having large changes in quantum number in the out-of-plane bending modes. This enables these modes to serve as accepting modes and enhances the internal conversion rate. However, even Villa *et al.* acknowledge that this explanation is also problematical, as a large geometry change would result in extensive vibrational activity in the displaced modes, which is not seen.

Had the proximity effect been an acceptable explanation for the photophysics of pyridine, some other mechanism would be required to explain the tetrazine data. The proximity effect requires a small energy separation between the initially excited $\pi^* \leftarrow n$ state and the higher lying $\pi^* \leftarrow \pi$ state responsible for the effect. In pyridine this gap is 3500 cm^{-1} , while in tetrazine it is larger.⁵² The fact that amino substitution reduces the nonradiative rate in both cases would be hard to explain. In 2-aminopyridine, the lowest excited singlet state is the $\pi^* \leftarrow \pi$ state.⁵³ Although the argument is somewhat strained, one might postulate that amino grouped substitution lowers the $\pi^* \leftarrow \pi$ state so much that it inverts the excited states and the energy gap actually increases upon amino substitution. However, this argument completely fails in the case of tetrazine and AT since the lowest excited singlet state of AT is known to be the $\pi^* \leftarrow n$ state.²³

The final conclusion of Villa *et al.* that "Clearly, we are still far away from achieving proper understanding of the photophysics of [pyridine]" might be applied to tetrazine as well. There are similarities in the photophysics of the two molecules which suggest that the factors influencing the internal conversion rates in pyridine and its derivatives is likely to account for similar data in the tetrazine systems.

ACKNOWLEDGMENTS

This work was supported by NSF Grant No. CHE-8818321. J.C.A. gratefully acknowledges support under the National Science Foundation Graduate Fellowship Program. S.J.M. acknowledges support from the Illinois Minority Graduate Incentive Program, and from the Dorothy Danforth Compton Fellowship Program. We are indebted to Dr. D. D. Yang for providing us with the samples of AT and AMT. We acknowledge Professor E. C. Lim for a helpful conversation. We thank Dr. Graham Fleming for providing us with computer programs for fitting the fluorescence lifetimes.

¹D. V. Brumbaugh and K. K. Innes, *Chem. Phys.* **59**, 413 (1981).

- ²K. K. Innes, L. A. Franks, A. J. Merer, G. K. Vemulapalli, T. Cassen, and J. Lowry, *J. Mol. Spectrosc.* **66**, 465 (1977).
- ³X. Zhao, W. B. Miller, E. J. Hints, and Y. T. Lee, *J. Chem. Phys.* **90**, 5527 (1989).
- ⁴R. E. Smalley, L. Wharton, D. H. Levy, and D. W. Chandler, *J. Mol. Spectrosc.* **66**, 375 (1977).
- ⁵D. V. Brumbaugh, C. A. Haynam, D. H. Levy, *J. Mol. Spectrosc.* **94**, 316 (1982).
- ⁶A. C. Scheiner and H. F. Schaefer III, *J. Chem. Phys.* **87**, 3539 (1987).
- ⁷A. C. Scheiner, G. E. Scuseria, and H. F. Schaefer III, *J. Am. Chem. Soc.* **108**, 8160 (1986).
- ⁸R. M. Hochstrasser and D. S. King, *Chem. Phys.* **5**, 439 (1974).
- ⁹R. M. Hochstrasser and D. S. King, *J. Am. Chem. Soc.* **97**, 4760 (1975); **98**, 5443 (1976).
- ¹⁰J. R. McDonald and L. E. Brus, *J. Chem. Phys.* **59**, 4966 (1973).
- ¹¹J. H. Meyling, R. P. vanderWerf, and D. E. Wiersma, *Chem. Phys. Lett.* **28**, 364 (1974).
- ¹²R. M. Hochstrasser, D. S. King, and A. B. Smith, *J. Am. Chem. Soc.* **99**, 3923 (1977).
- ¹³P. F. Barbara, L. E. Brus, and P. M. Rentzepis, *Chem. Phys. Lett.* **69**, 447 (1980).
- ¹⁴T. J. Aartsma, W. H. Hesselink, and D. A. Wiersma, *Chem. Phys. Lett.* **71**, 424 (1980).
- ¹⁵A. Kiermeier, K. Dietrich, E. Riedle, and H. J. Neusser, *J. Chem. Phys.* **85**, 6983 (1986).
- ¹⁶J. F. Ramaekers, thesis, University of Amsterdam, 1983.
- ¹⁷M. Chowdhury and L. Goodman, *J. Chem. Phys.* **38**, 2979 (1963).
- ¹⁸G. K. Vemulapalli and T. Cassen, *J. Chem. Phys.* **56**, 5120 (1972).
- ¹⁹J. Langelaar, D. Bebelaar, M. W. Leeuw, J. J. F. Ramaekers, and R. P. H. Rettschnick, in *Proceedings, 2nd International Conference of Pico-second Phenomena* (Springer, Berlin, 1980), p. 147.
- ²⁰J. DeVries, D. Bebelaar, and J. Langelaar, *Opt. Commun.* **18**, 24 (1976).
- ²¹C. A. Haynam, L. Young, C. Morter, and D. H. Levy, *J. Chem. Phys.* **81**, 5216 (1984).
- ²²J. C. Alfano, S. J. Martinez III, and D. H. Levy, *J. Chem. Phys.* **91**, 7302 (1989).
- ²³J. C. Alfano, S. J. Martinez III, and D. H. Levy, *J. Mol. Spectrosc.* **143**, 366 (1990).
- ²⁴J. C. Alfano, S. J. Martinez III, and D. H. Levy, *J. Chem. Phys.* **94**, 1673 (1991).
- ²⁵D. V. Brumbaugh, C. A. Haynam, and D. H. Levy, *J. Mol. Spectrosc.* **94**, 316 (1982).
- ²⁶M. E. Carrasquillo, T. S. Zwier, and D. H. Levy, *J. Chem. Phys.* **83**, 4990 (1985).
- ²⁷M. C. Chang, S. H. Courtney, A. J. Cross, R. J. Gulotty, J. W. Petrich, and G. R. Fleming, *Anal. Inst.* **14**, 433 (1985).
- ²⁸H. H. Takimoto and C. C. Denault, *Tetrahedron Lett.* **44**, 5369 (1966).
- ²⁹A. D. Counotte-Potman and H. C. vanderPlass, *J. Heterocyclic Chem.* **15**, 445 (1987).
- ³⁰S. F. Mason, *J. Chem. Soc.* **1959**, 1263.
- ³¹M. W. Leeuw, thesis, University of Amsterdam, 1981.
- ³²J. Strickler and R. A. Berg, *J. Chem. Phys.* **37**, 814 (1963).
- ³³J. B. Birks, *Photophysics of Aromatic Molecules* (Wiley-Interscience, London, 1970), pp. 87-88.
- ³⁴R. A. Lampert, S. R. Meech, J. Metcalfe, D. Phillips, and A. P. Schaap, *Chem. Phys. Lett.* **94**, 137 (1982).
- ³⁵G. Hug and R. S. Becker, *J. Chem. Phys.* **65**, 55 (1976).
- ³⁶J. R. Andrews and B. S. Hudson, *J. Chem. Phys.* **68**, 4587 (1978).
- ³⁷T. Shibuya, *Chem. Phys. Lett.* **103**, 46 (1983).
- ³⁸B. A. Jacobson, J. A. Guest, F. A. Novak, and S. A. Rice, *J. Chem. Phys.* **87**, 269 (1987).
- ³⁹R. Scheps, D. Florida, and S. A. Rice, *J. Chem. Phys.* **61**, 1730 (1974).
- ⁴⁰I. Yamazaki, M. Fujita, and H. Baba, *Chem. Phys.* **57**, 431 (1981).
- ⁴¹A. E. W. Knight and C. S. Parmenter, *Chem. Phys.* **15**, 85 (1976).
- ⁴²I. Yamazaki, T. Murao, T. Yamanaka, and K. Yoshihara, *Faraday Discuss. Chem. Soc.* **75**, 395 (1983).
- ⁴³I. Yamazaki, K. Sushida, and H. Baba, *J. Chem. Phys.* **71**, 381 (1979).
- ⁴⁴K. Sushida, M. Fujita, I. Yamazaki, and H. Baba, *Bull. Chem. Soc. Japan* **56**, 2228 (1987).
- ⁴⁵J. W. Hager and S. C. Wallace, *J. Phys. Chem.* **89**, 3833 (1985).
- ⁴⁶J. W. Hager, G. W. Leach, D. R. Demmer, and S. C. Wallace, *J. Phys. Chem.* **91**, 3750 (1987).
- ⁴⁷R. M. Hochstrasser and C. A. Marzocco, in *Molecular Luminescence*,

- edited by E. C. Lim (Benjamin, New York, 1969), p. 631.
- ⁴⁸W. A. Wassam, Jr. and E. C. Lim, *J. Chem. Phys.* **68**, 433 (1978). in R. M. Hochstrasser and C. A. Marzzacco, in *Molecular Luminescence*, edited by E. C. Lim (Benjamin, New York, 1969), p. 631.
- ⁴⁹E. C. Lim, in *Excited States*, edited by E. C. Lim (Academic, New York, 1977), Vol. 3, p. 305.
- ⁵⁰E. C. Lim, *J. Phys. Chem.* **90**, 6770 (1986).
- ⁵¹E. Villa, A. Amirav, and E. C. Lim, *J. Phys. Chem.* **92**, 5393 (1988).
- ⁵²A. C. Scheiner and H. F. Schaefer III, *J. Chem. Phys.* **87**, 3539 (1987).
- ⁵³J. M. Hollas, G. H. Kirby, and R. A. Wright, *Mol. Phys.* **18**, 327 (1970).